IN-1112
August 1967

CHARACTERIZATION OF THE FRACTURE SURFACE OF THE PM-2A PRESSURE VESSEL

W. F. Zelezny and J. M. Beeston

IDAHO NUCLEAR CORPORATION
NATIONAL REACTOR TESTING STATION
IDAHO FALLS, IDAHO

U. S. ATOMIC ENERGY COMMISSION

DISCLAIMER

Printed in the United States of America
Available from
Clearinghouse for Federal Scientific and Technical Information
National Bureau of Standards, U. S. Department of Commerce
Springfield, Virginia 22151
Price: Printed Copy $3.00; Microfiche $0.65

LEGAL NOTICE

IN-1112
Issued: August 1967
Radiation Effects on Materials
TID-4500

CHARACTERIZATION OF THE FRACTURE SURFACE OF THE PM-2A PRESSURE VESSEL

By

W. F. Zelezny and J. M. Beeston

IDAHO NUCLEAR CORPORATION

A JOINTLY OWNED SUBSIDIARY OF
AEROJET GENERAL CORPORATION
ALLIED CHEMICAL CORPORATION

U. S. Atomic Energy Commission Research and Development Report
Issued Under Contract AT(10-1)-1230
Idaho Operations Office

ACKNOWLEDGEMENTS

Particular acknowledgement is extended to C. D. Beachem for his comments on the analysis and to Clyde May for performing the replication and electron microscopy. Thanks are due also to the TAN Hot Cell personnel under the direction of D. R. Alvord who rendered valuable assistance in making this examination possible.

ABSTRACT

CHARACTERIZATION OF THE FRACTURE SURFACE
OF THE PM-2A PRESSURE VESSEL

By
W. F. Zelezny and J. M. Beeston

The PM-2A pressure vessel, which in service had received a fluence of the order of 10^{19} neutrons/cm^2, was tested in a controlled fracture mechanics program with the intent of producing a brittle failure. The destructive test condition of -20°F insured that the failure took place well below the NDT temperature of the irradiated A350 - LF3 steel. The resulting fracture originated in an elongated artificial defect and extended axially along the cylindrical wall of the pressure vessel from both ends of the defect.

A 21 inch length of fracture surface, including the artificial defect, was obtained for the purpose of characterizing the fracture and estimating the percentage of brittle fracture (1) by over all macro-observation of the fracture appearance, (2) by electron fractography, and (3) by examination of the microstructure of the adjacent material to determine composition, grain size, and inclusion frequency or soundness.

Four distinct regions were observed, namely (1) a shear lip in the A350 - LF3 steel along the outside edge of the pressure vessel, (2) the fracture through the 304 stainless steel weld deposit which formed a liner for the vessel, (3) the stress corrosion region which started at the tip of the artificial defect and extended an appreciable distance into the A350 - LF3 steel, and (4) the rapid running fracture which comprised by far the major portion of the fracture surface in the A350 - LF3 steel. Extensive dimpling in the shear lip and in the 304 stainless steel liner indicated the fracture was ductile in these regions (estimated at less than 10% brittle). A stress corrosion region at the base of the artificial defect was surprisingly deep and showed mostly corrosion products with few clear cut indications of cleavage planes. Fractographs from the region of the rapid running fracture, regardless of whether at the fracture origin or at points at varying distances from the origin, showed principally quasi-cleavage. This extensive quasi-cleavage and the overall macro-observations led to an estimate of at least 90% brittle fracture for the rapid running fracture.

SUMMARY

The following conclusions are made from the results of the examination of the fracture surface:

1. The conditions of test designed to produce a brittle failure were successful in that a flat running crack extended from the crack origin at the end of the artificial defect to the top and bottom closure flanges. The flat crack (interior region of A350 - LF3 steel) in the 21 inch region examined exhibited a degree of brittleness in excess of 90%. Electron fractographs from the interior fracture surface examined showed the same characteristic, namely quasi-cleavage.

2. The depth of the stress corrosion region (0.16 to 0.20 inch) observed was three to four times as great as calculated from an experimental rate of 0.025 inches per hour.

3. A shear lip on the outer diameter of the vessel was principally due to relaxation of the stress at the surface, however the magnitude (0.1 inch wide and deep with a slight plastic contraction) may have been partly due to lowered embrittlement in the outer vessel diameter.

4. The thickness (0.30 to 0.33 inches) of the stainless steel weld overlay was greater than the specified minimum thickness of 3/16 inch, which may have contributed to the difficulty of starting the crack.

5. The A350 - LF3 steel appeared relatively free of inclusions and was fine grained with grain size estimated by the ASTM comparative method as No. 8.

6. Fractographs of the stainless steel and shear lip regions showed dimpling characteristic of a ductile fracture.

CONTENTS

FIGURES

TABLES

I. INTRODUCTION

A primary aim in the design of nuclear power plants is the avoidance of brittle fracture of the highly pressurized components of the system. The low alloy, structural steels commonly used in the outer walls of reactor pressure vessels will show brittle behavior below certain temperatures known as the NDT (nil ductility transition) temperatures which become higher as the irradiation dosage of the steels is increased. It was of great interest to the designers of reactor pressure vessels to be able deliberately to produce a brittle failure in such a vessel after it had been irradiated in service. Such an opportunity came when the PM-2A power reactor, after providing electrical energy for nearly three years for the U.S. Army installation at Camp Century in Greenland, was shut down in July, 1963, for disassembly.

The overall objective of this test was to produce a failure by brittle fracture of the irradiated reactor vessel under a set of known conditions. It is anticipated that the results of the test will lead to a better understanding of the conditions necessary for a brittle fracture of an operating reactor pressure vessel to occur and to more exact specifications for reactor pressure vessel design. The objective of the investigation described in this report was the characterization of the fracture surface produced by the destructive test of the PM-2A pressure vessel.

The outer shell of the PM-2A pressure vessel consisted of A350 - LF3 steel with a specified thickness of 2.375 inches. The liner of the pressure vessel was a 304 stainless steel weld deposit with a specified minimum thickness of 0.1875 inch. Actually, the thickness of the stainless steel was somewhat greater, varying between 0.30 and 0.33 inches.

The literature[1, 2] describes in detail how the pressure vessel of this reactor was tested to destruction at the National Reactor Testing Station in Idaho. The procedure included pressurization of the vessel with an increasingly large artificial defect and also cyclic pressurization of the vessel with the intended purpose of producing fatigue damage which would assist in the production of a failure.

In order to insure that the fracture produced by failure was initiated at a desired location of the pressure vessel and also was a brittle fracture an artificial defect was produced in the wall of the vessel (see Figure 1) covering the region of maximum irradiation dosage. The defect was produced in two steps by means of electrical discharge machining. The first step used a vee-shaped (30° angle) carbon electrode to produce an elongated indentation of triangular cross-section. The second step employed a 0.001 inch thick tungsten foil electrode to introduce a hairline slot approximately 0.030 inch deep at the tip of the vee-shaped defect. The initial defect was 3/8 inch deep by 3 inches long and, in the time interval between vessel pressurizations, was increased stepwise in size to the final dimensions of 1-3/4 inches deep by 11 inches long.

Pressurization to 5250 psi at -20°F with the large defect present, including several hundred cyclic pressurizations in an attempt to introduce fatigue damage, did not produce failure. Accordingly, resort was made to stress corrosion cracking to sharpen and deepen the root of the defect.

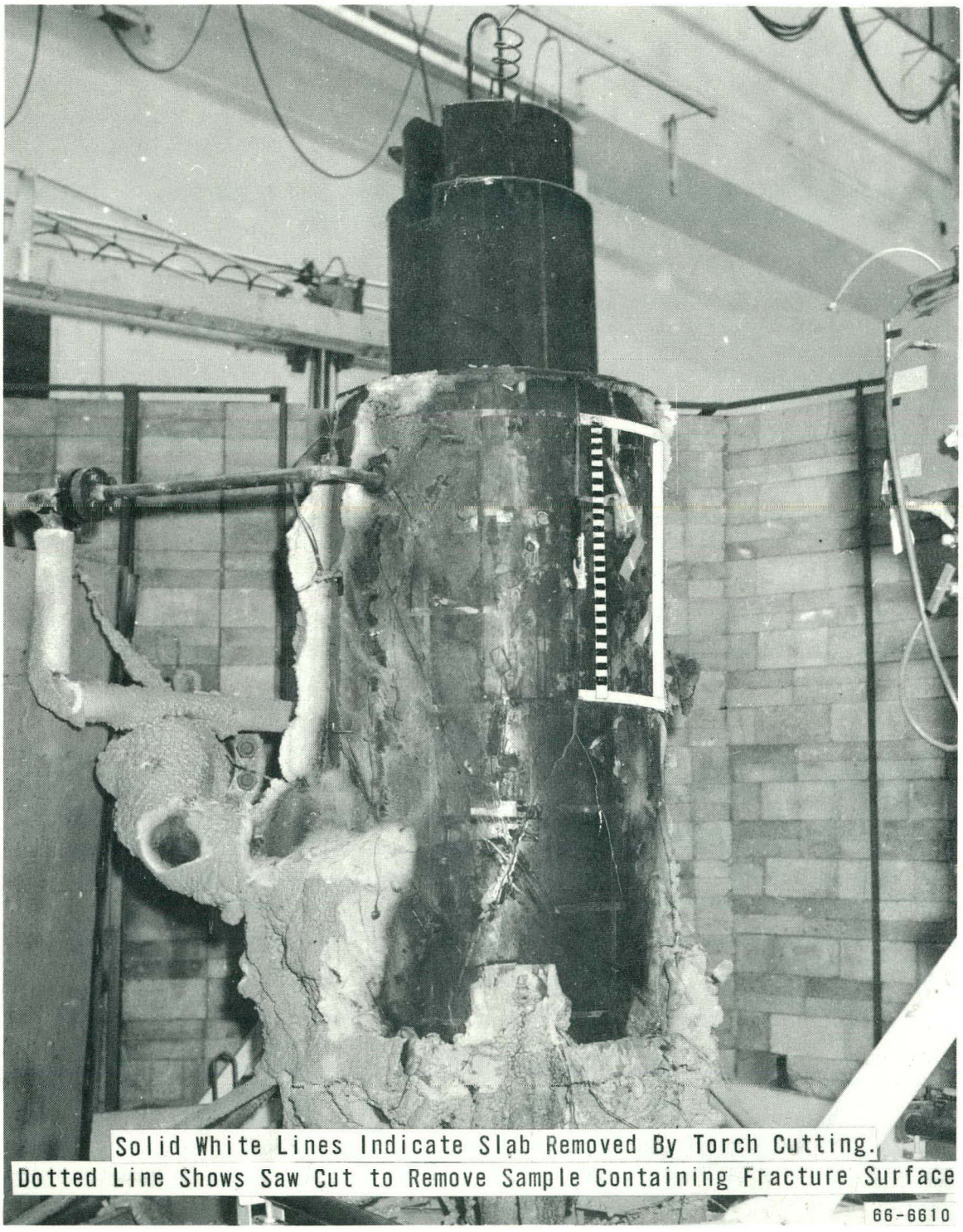

FIG 1.

Overall View of PM-2A Pressure Vessel, Showing Fracture Extending From Both Ends of Artificial Defect.

II. PROCEDURE

A. MACRO-PHOTOGRAPHY

Over 100 macrophotos, some at 3X and some at 10X, were taken so that the entire fracture surface was completely covered at 3X and all typical regions were sampled at 10X. Each picture was taken both in black and white and in color. Many of the photographs were stereo pairs.

B. REPLICATION TECHNIQUE

A two-stage replication technique was employed, with the first stage impression of the fracture surface obtained by remote application of the replicating solution and tape using manipulators in the TAN RML Hot Cell. A solution of cellulose acetate in dioxane was first applied to the desired area of the fracture surface, followed by a strip of cellulose acetate tape attached to a strip of stainless steel shim stock to provide a means of gripping the tape with the manipulators. A solution of cellulose acetate in acetone is normally used in this procedure. However, the temperature in the hot cell, due to the large number of lights used, was sufficiently high to cause boiling of the acetone, resulting in extensive bubbles in the replica. Accordingly, dioxane was substituted for the acetone and no more difficulty with bubbles was encountered. In order to produce the second stage of the replica, the cellulose acetate impressions thus obtained were shadowed at an angle of 25 degrees from the normal with 80% Pt - 20% Pd in a vacuum evaporator, followed by the deposition of a carbon film. The resulting cellulose acetate-(Pt-Pd)-carbon sandwich was cut in small squares and immersed in acetone to dissolve away the cellulose acetate, leaving the shadowed carbon replicas.

Each of the regions indicated in Figure 2 were replicated at least twice. The first cellulose acetate replica taken in each region served to clean the area by removing loose microscopic particulate material and was not used in preparing the second stage of the replica. The second (and cleaner) cellulose acetate replica was normally used for preparation of the second stage replica. Some areas were replicated as many as four times before satisfactory replicas were obtained.

An RCA EMU-3F electron microscope was used in the examination of these replicas. Over 200 electron fractographs were photographed, printed and used in the analysis.

C. SURFACE PREPARATION

Preparatory to examination of the surface it was washed several times with "Methachlor" and given a final rinse with acetone, since the surface was left covered with corrosion inhibiting oil as discussed in the next paragraphs.

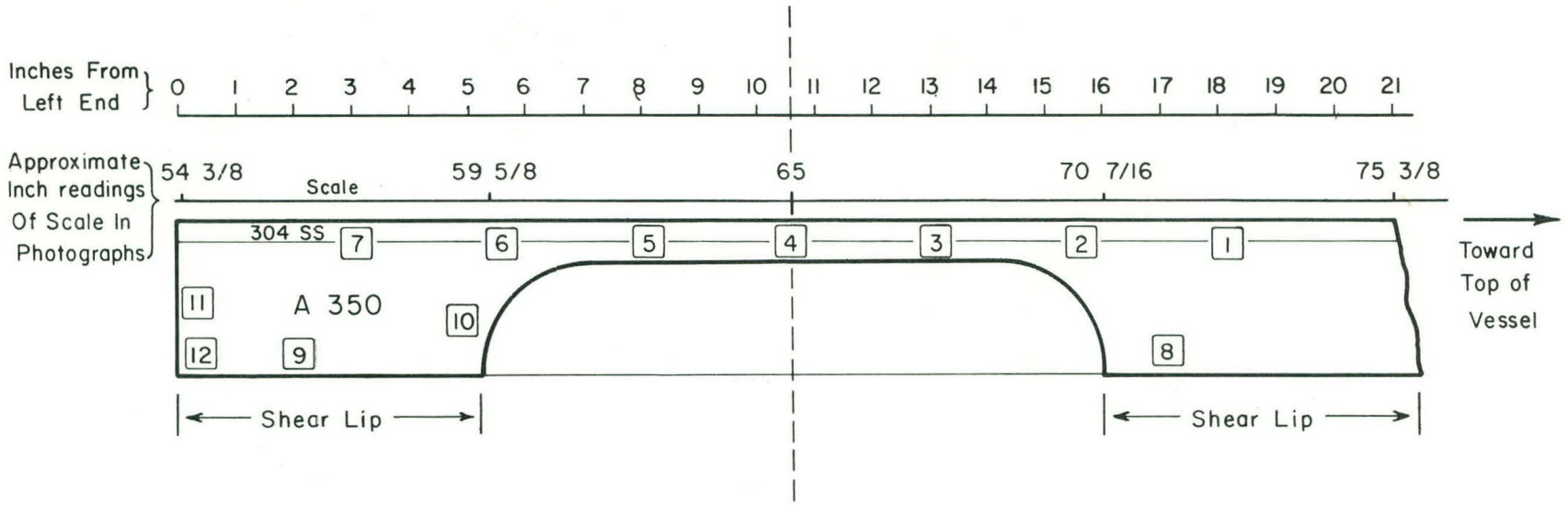

Sketch of Sampling Positions on Fracture Surface of PM-2A.

FIG. 2

In the first stress corrosion procedure the lower half of the defect was filled with a 1:1 HCl solution at 72°F held in place by a dam while the vessel was pressurized to 4000 psi. After one hour of this treatment the acid was flushed from the defect and another attempt to burst the vessel by pressurizing to 5250 psi at -20°F did not produce any damage. During a second stress corrosion treatment with the internal pressure raised to 5000 psi the crack-opening displacement measuring instrumentation indicated a wider opening than previously. This was taken as an indication of the presence of a stress corrosion crack. After again flushing out the acid the vessel was cooled to -20°F and pressurization commenced. A violent failure occurred at 4475 psi, producing the fracture illustrated in Figure 1. It will be noted that the fracture is a straight line extending upward from the defect to the top of the vessel and downward from the defect for about 18 inches at which point it divides into two branches.

At the instant of failure the hydraulic fluid with which the vessel was pressurized issued violently from the crack and undoubtedly covered the fracture surface, thus providing protection against corrosion. As a further precaution the fracture was sprayed with a corrosion inhibiting oil available in aerosol spray cans under the trade name, "Surface Shield". Either or both were effective in providing protection against corrosion since the fracture surface, except for the stress corroded surface, was clean and uncorroded when it became available for examination three months later.

A cutting torch was used to remove a slab shown in Figure 1 as bounded on three sides by the solid white line and by the fracture on the fourth side. A saw cut along the dotted line of Figure 1 produced a slice 2-1/2 inches wide carrying the fracture surface and one side of the artificial defect as illustrated in Figure 3A. The results of the examination of this fracture surface constitute the subject of this report.

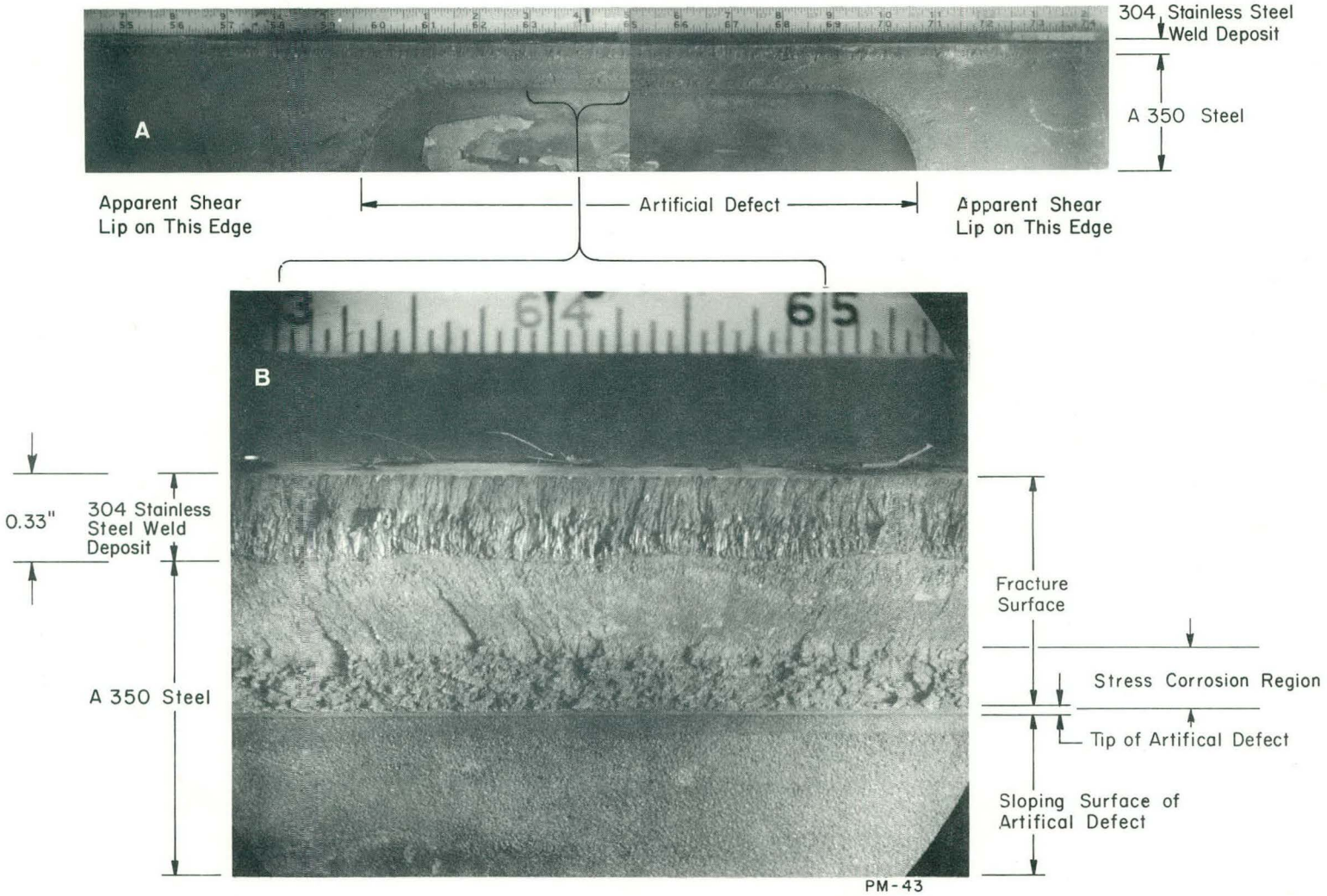

Figure 3 (A) Overall View of Fracture Surface Including Artificial Defect. (B) Magnified View (3x) of Region Containing Origin of Fracture. Note the "chevron" Lines Sloping Toward the Origin of the Fracture and the Jagged Tear Region Next to the Artificial Defects, and that the Chevron Lines do not Penetrate the Stress Corrosion Region.

III. GENERAL APPEARANCE OF FRACTURE SURFACE AND EXPERIMENTAL FINDINGS

A. MACRO-APPEARANCE

The fracture surface shown in Figure 3A is reproduced at higher magnification by means of the composite pictures reproduced in Figure 4. Figure 3B is an enlargement of the region in which the rapid running crack must have started, as attested to by the oppositely sloping chevron marks which slope toward the origin of the crack.

Figure 5 is a tracing of part of Figure 3A with several regions of interest delineated. Along the top edge beyond each end of the artificial defect are shear lips, an example of which is shown in Stereo in Figure 6 and in profile in Figure 7. This stereo figure and the ones to follow are reproduced in such a manner as to benefit readers who may wish to remove the illustrations from the report for observation in a stereo viewer. Of special interest is the corroded region indicated by cross-hatching. Considerable evidence will be presented later in this report to show that it is the region composed largely of stress corrosion cracking, and that the stress corrosion cracking went to a surprisingly great depth. This region is characterized by a corroded surface having the usual brownish color of oxidized iron. Most of this same corroded surface has a distinctly rougher, "mountainous" topography which seems to be associated with the stress corrosion cracking. The remainder of the fracture showed the dark gray color normally associated with uncorroded steel fracture surfaces and in general was less rough in topography than the stress corrosion region, with the possible exception of the 304 stainless steel weld deposit which showed a coarse, distinctly columnar grain structure next to the underlying A350 - LF3 steel.

B. REGION OF STRESS CORROSION

Several pieces of evidence were used in finally assigning a boundary to the extent of the stress corrosion cracking which preceded the final destructive test. Visual observation and color photographs revealed a region characterized by the reddish-brown color of oxidized iron, roughly outlined by the dotted line in the tracing, Figure 5. It will be noted in Figure 4 as indicated in Figure 5 that the oxidized surface is most extensive in the lower end of the artificial defect and tapers to almost nothing at the upper end. Almost all of the "rusty" area also showed a distinct roughness ("mountains and valleys") most clearly observable and impressive if Figure 8 is viewed in stereo. Still another experimental observation is the fact that the chevron marks (one is shown in Figure 8) do not enter the rough region.

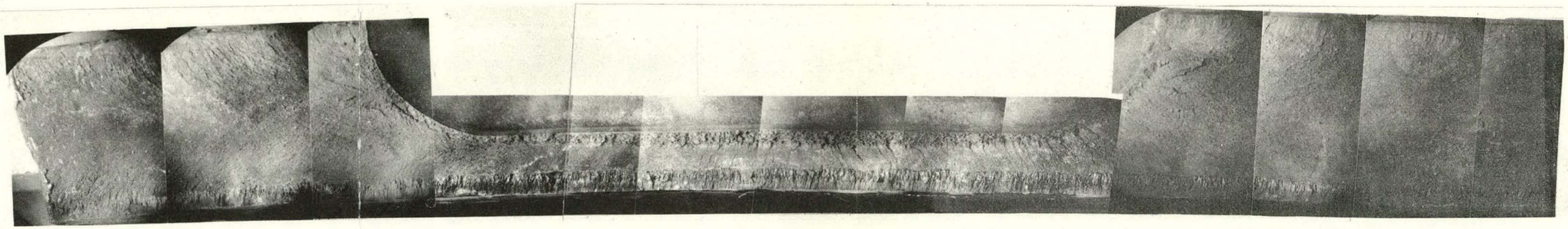

67-3344, 3345

Composite View Showing Fracture Surface, Including Artificial Defect.

FIG 4.

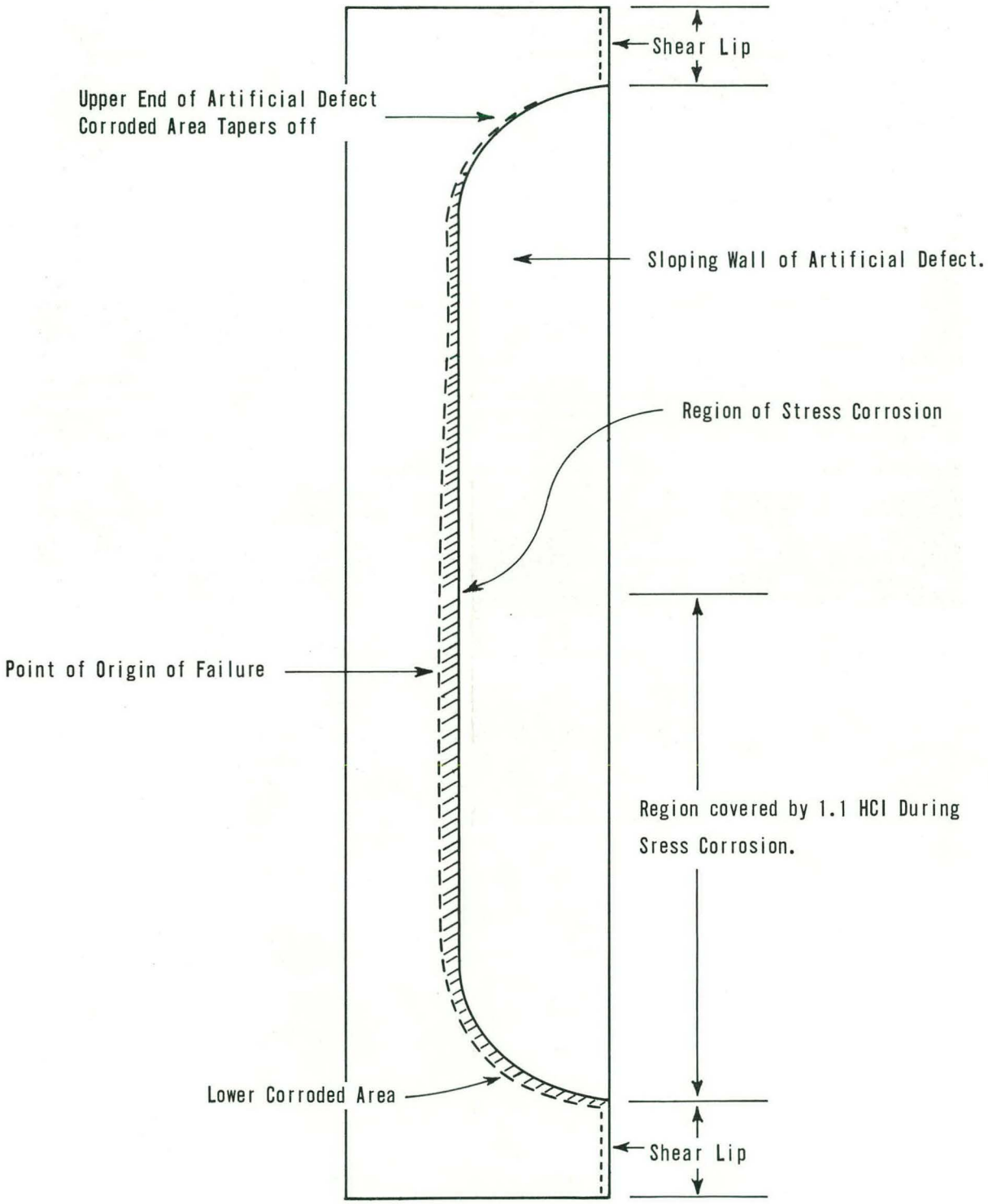

Tracing of Artificial Defect and Crack Origin Region

Fig 5.

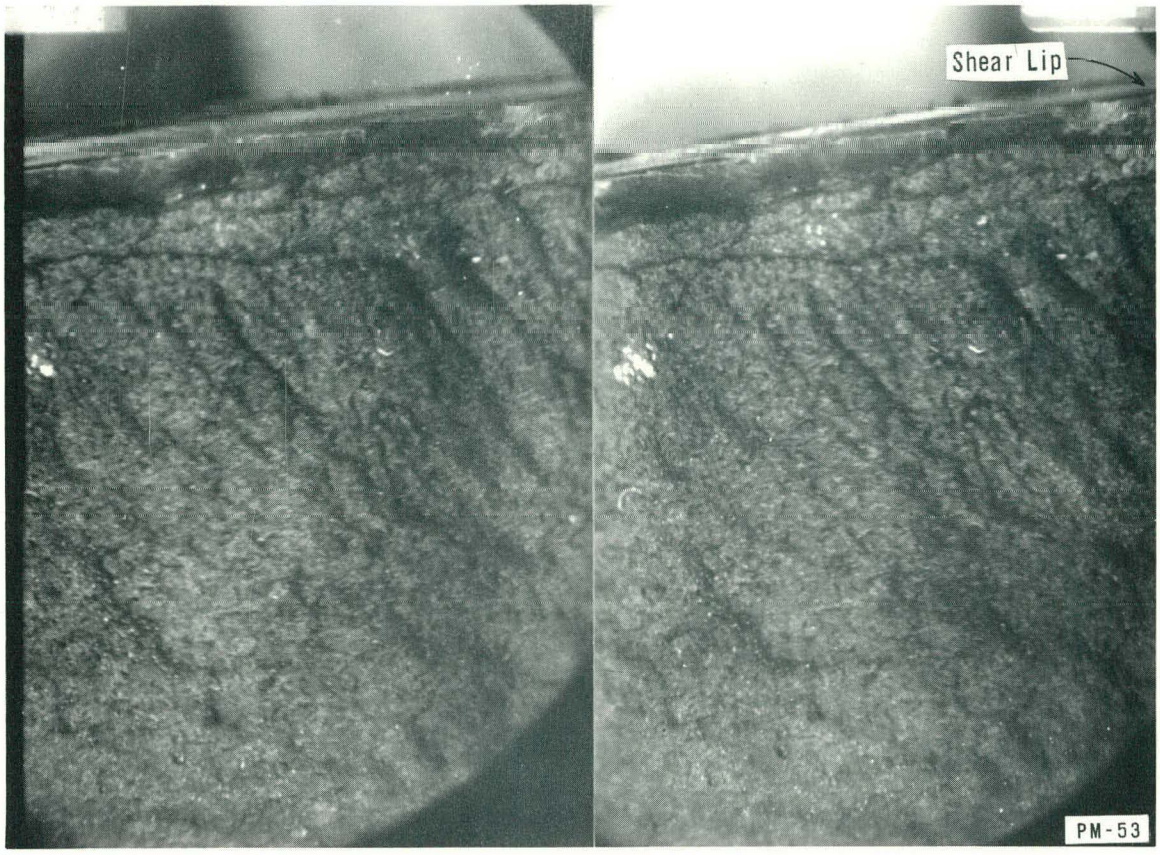

FIG 6. Stereophotograph of Shear Lip. 3 x

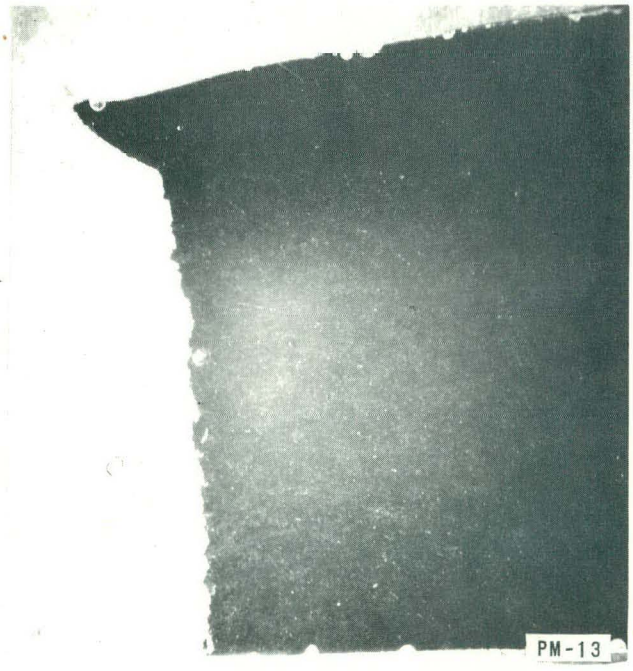

FIG 7. Profile of Shear Lip 6.5 x

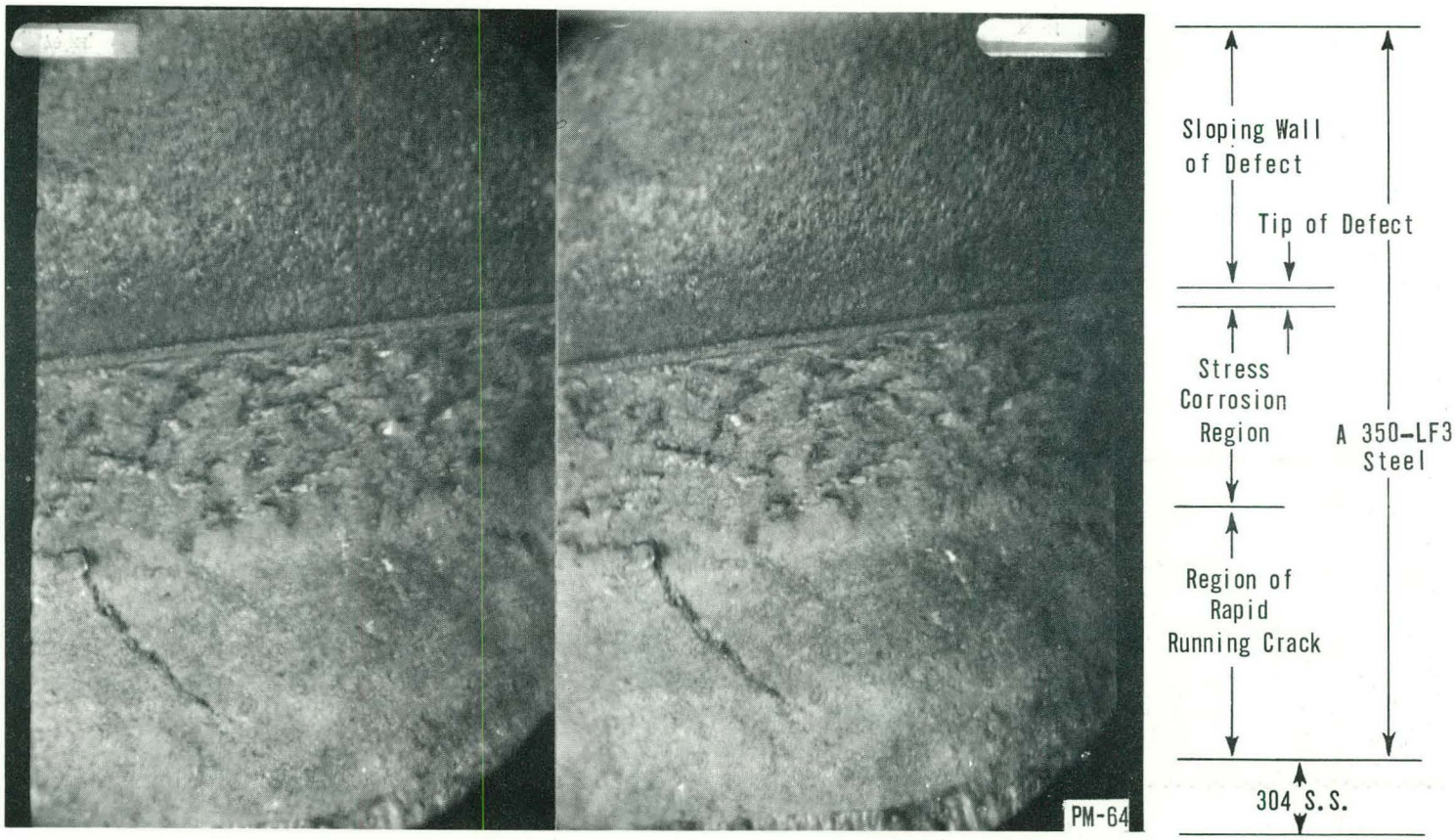

Stereophotograph of Fracture Surface, Showing Defect, Stress Corrosion Region, Rapid Running Crack and Edge of Stainless Steel Liner. Note That Chevron (Lower Left Hand Quadrant of Photo) Does Not Enter Stress Corrosion Region. 3 x

FIG 8.

The chevron marks are features produced by the rapid running fracture which burst the vessel. This rapid running fracture which occurred after the stress corrosion crack had been produced necessarily started at the tip of the crack caused by the stress corrosion. Accordingly, the chevron marks could not be expected to be found in the region of stress corrosion cracking and are useful in distinguishing between the stress corrosion and rapid crack regions. On this basis it was decided that the rough region outlined approximately in Figure 5 was indeed the area of stress corrosion cracking.

An additional and clinching piece of evidence for determining the extent of the stress corrosion is the metallographic cross section of Figure 9A which illustrates a transverse profile of part of the artificial defect and part of the fracture surface about two inches below the point of origin of the rapid running fracture. From top to bottom it shows the sloping wall of the artificial defect, the tip of the defect, a rough surface penetrated by several cracks and, finally a smoother surface. The enlarged view of some of the cracks (Figure 9B) shows them to have the characteristic appearance of stress corrosion cracks from which it is concluded that the rough surface is one side of the main stress corrosion crack while the small cracks are branches of the main corrosion crack. The depth of the stress corrosion crack on this illustration is 0.16 inches. Examination of macro-photographs of the fracture surface indicates that in many places 0.20 inches is a more appropriate figure, and that 0.16 inches may be a slightly low estimate of the crack depth. The smoother surface below the stress corrosion crack wall is the region of the rapid running fracture.

During the production of the stress corrosion crack the 1:1 HCl solution was held in place by a dam which covered only the lower half of the defect. The stress corrosion crack, however, was observed to extend almost the full length of the artificial defect. This may be explained by assuming that the acid solution traveled upward along the bottom of the tip of the artificial defect by capillary action, hence the stress corrosion was not confined to the locale of the dam.

The rusty appearance in some places appears to extend slightly beyond the rough area of stress corrosion cracking. An explanation for this is the probability that the acid contained in the stress corrosion crack would not be removed effectively by the rinse due to the difficulty of flushing out such a narrow crack and could have crept somewhat along the surface of the metal after the final rupture.

C. WELD OVERLAY

Optical metallography of the stainless steel revealed two distinct regions, as indicated in stereo in Figure 10 and by the photomicrographs in Figure 11 which show long columnar grains adjacent to the A350 steel, a rather sharp interface between a region of coarse grain and a region of finer, probably dendritic, grains in the stainless steel. The finer grain structure extended all the way to the free edge of the stainless steel. In general the boundary between the stainless steel weld deposit and the underlying A350 steel was sharp, distinct and free of welding flaws. The two regions of differing grain size within the stainless steel may be an indication that the weld was deposited in two layers. A thickness of 0.30 to 0.33 inches of the stainless steel was measured in several places in the region examined which may have contributed to the difficulty of starting the crack.

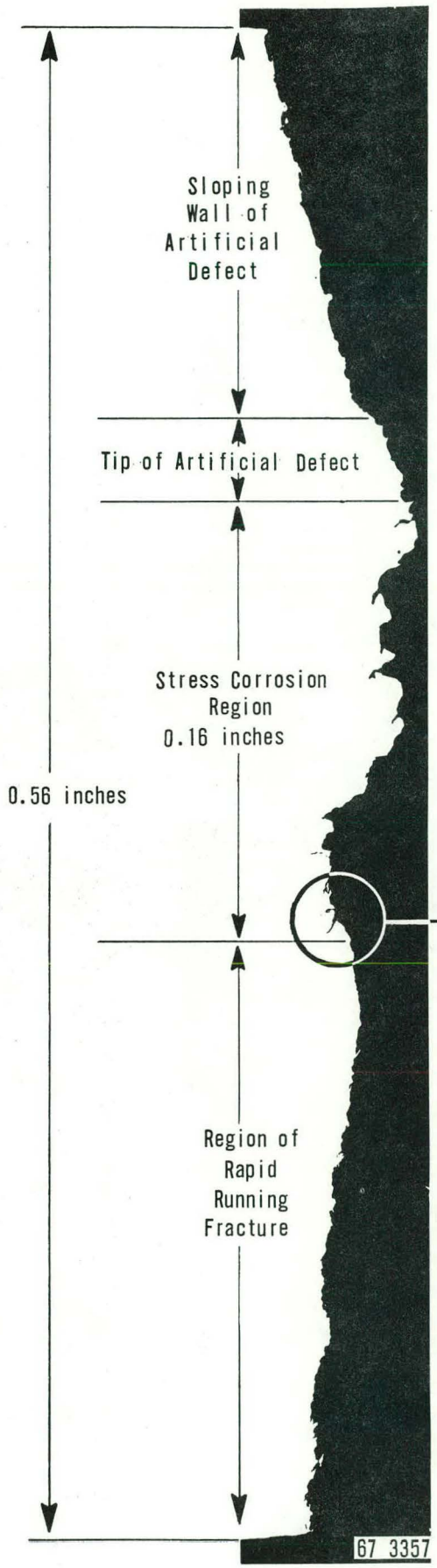

A. Profile of Part of Articial Defect and Fracture Surface, Including Sloping Wall and Tip of Articial Defect, Stress Corrosion Region and part of Rapid Running Fracture.

B. Photomicrograph of a few of the Branching Stress Corrosion Cracks.

FIG 9.

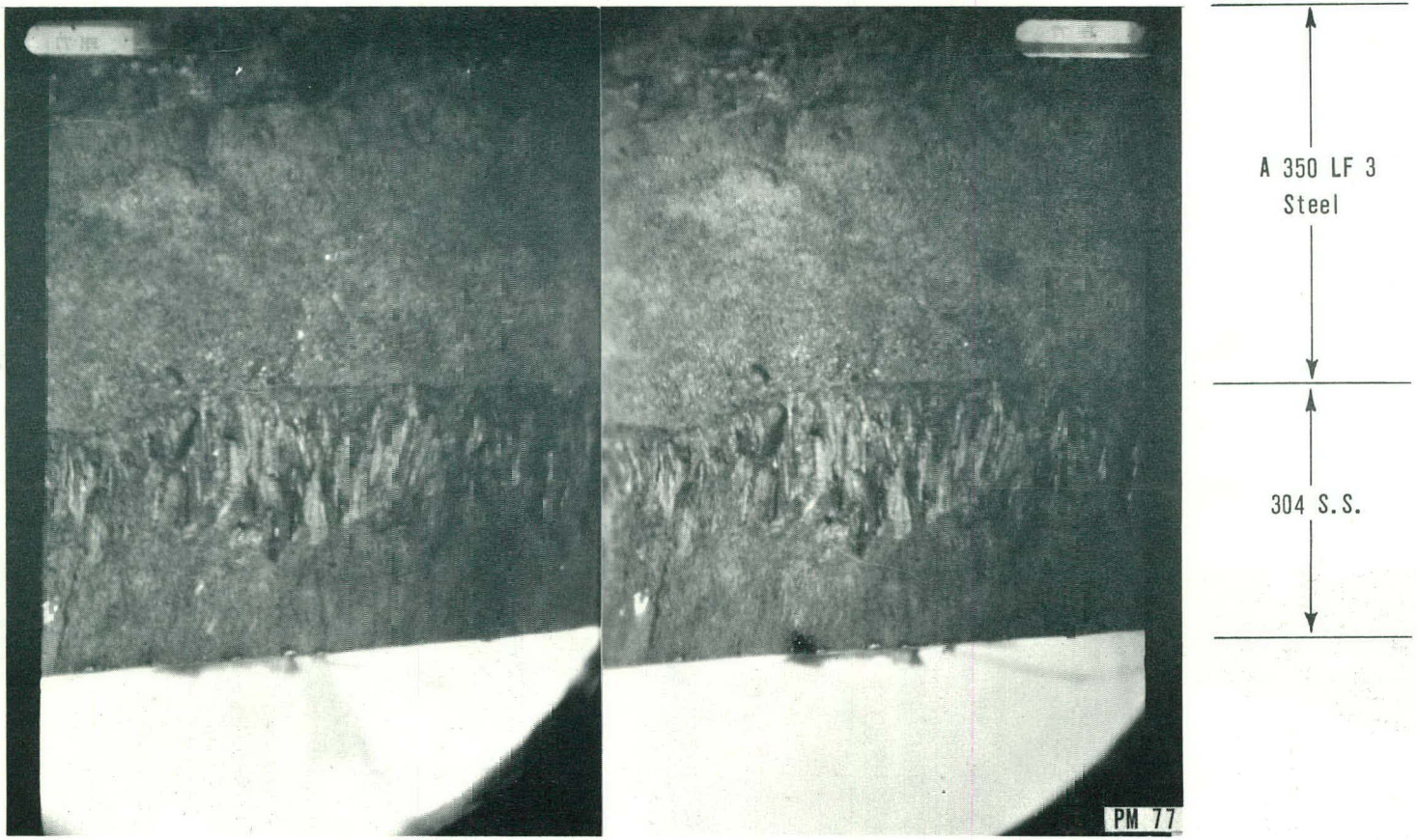

Stereophotograph of Fracture Surface Across Stainless Steel Weld Deposit.
Note Faint Traces of Shear Lip.

FIG 10.

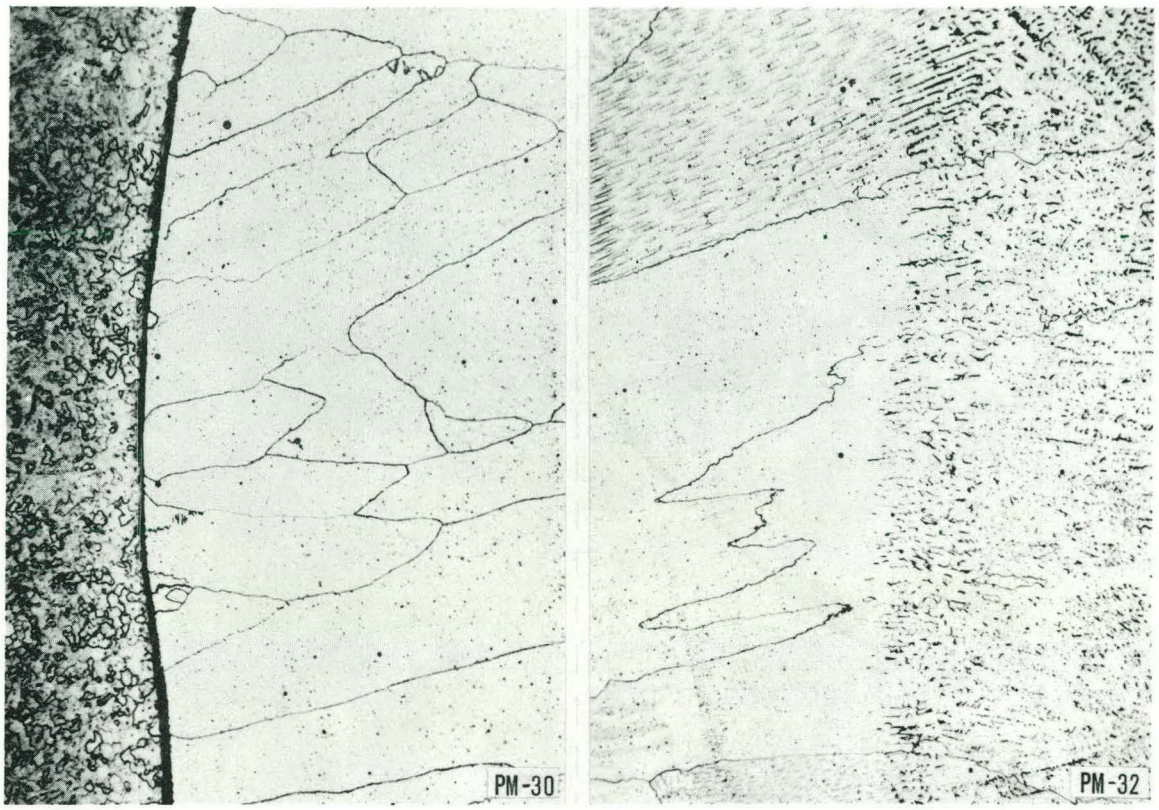

A. Boundary Between A 350 LF 3 Steel and 304 Stainless Steel, With Large Columnar Grains in the 304 S.S.

B. Boundary Between Two Regions of 304 S.S.

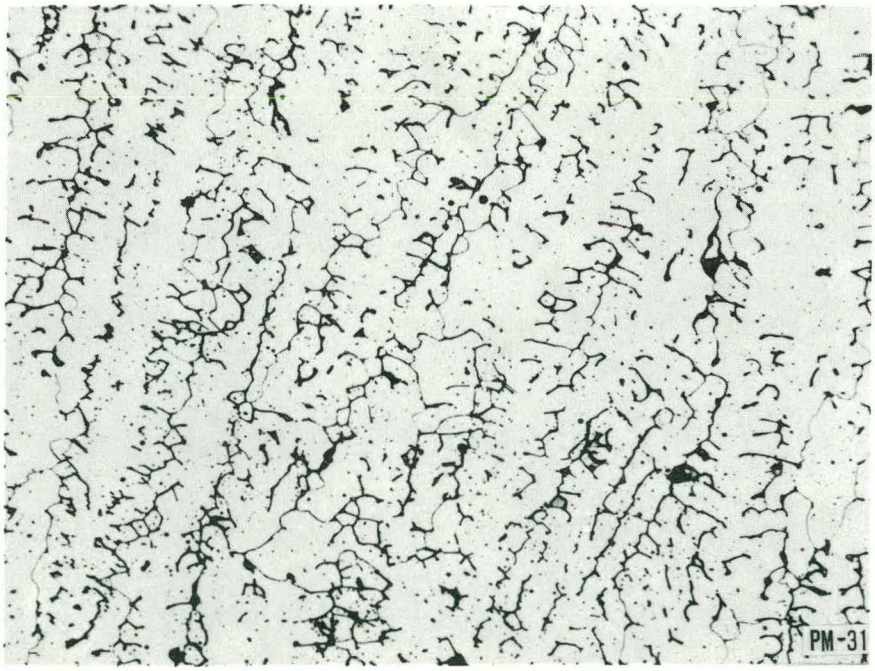

C. Finer Grained Dendritic Structure of Outer Layer of 304 S.S.

Photomicrographs of 304 Stainless Steel Weld Area. Oxalic Acid Etch. 200 x.

FIG 11.

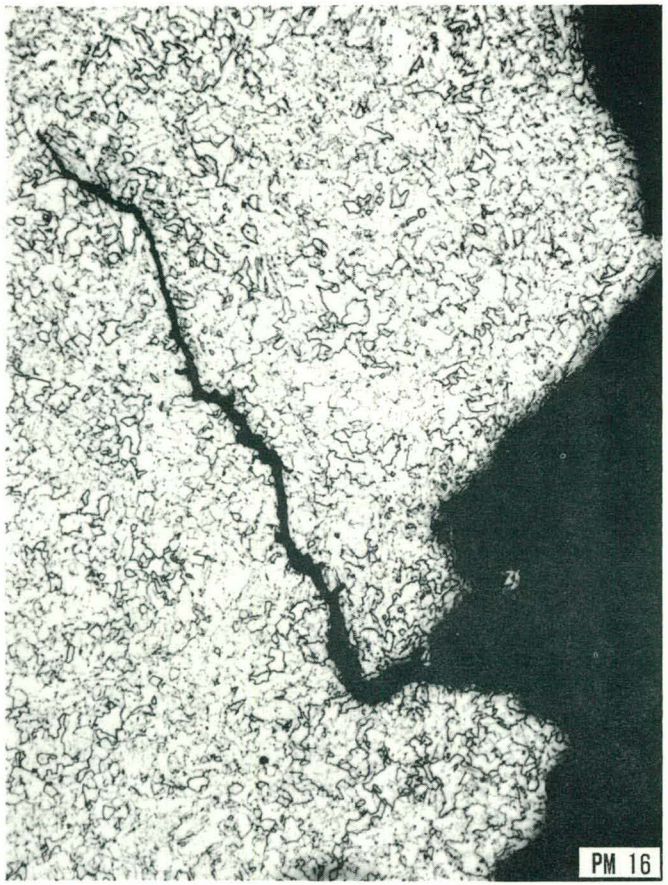

A. A Region Free of Inclusions. A Stress Corrosion Crack is Present. Nital Etch. 200 x.

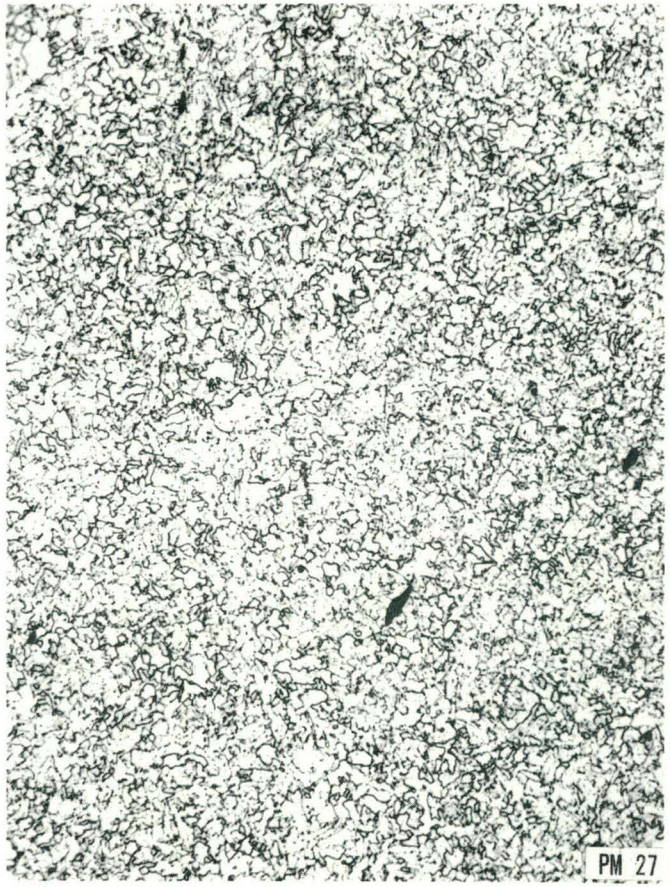

B. A Region Containing Typical Inclusions, Nital Etch. 200 x.

Microstructure of A 350–LF3 Steel.

FIG 12.

D. MICROSTRUCTURE AND CLEANLINESS OF A350 - LF3 STEEL

Microscopic observation of the polished and etched surfaces of the A350 steel revealed that it was quite clean and had relatively few inclusions. It was easy to find fields of view in the microscope at 200X which contained no inclusions. For example, the view of the A350 steel which fills part of the field in Figure 11A is completely free of inclusions, as is Figure 12A, also. Figures 9B and 12B show inclusions typical of those that were found. These same figures show the microstructure of the A350 steel which was relatively fine grained (ASTM grain size 8) with grains of irregular outline and some variation in grain size.

E. CHEMICAL COMPOSITION

Samples taken from the A350 steel wall and from the 304 stainless steel liner were analyzed chemically to determine whether the actual compositions of the steels were within the nominal specification limits. The results are listed in Table I, together with the specified compositions. Except for the high carbon analysis of the stainless steel, the steels seem to be within or very close to the specification limits.

TABLE I

SPECIFIED AND ANALYTICALLY DETERMINED COMPOSITION
OF STEELS IN PM-2A PRESSURE VESSEL

A. A350-LF3 STEEL

Element	Found by Analysis, wt%	Specified, wt%
C	0.17	0.20 max
Mn	0.53	0.90 max
P	0.032	0.04 max
S	0.03	0.04 max
Si	0.24	0.15 to 0.35
Ni	3.36 ± 0.15	3.25 to 3.75
Cu	0.14	
V	0.035	
Fe	95.98 ± 1.05	

B. 304 STAINLESS STEEL

Element	Analysis, wt%	Specified, wt%
C	0.219	0.08 max
Ni	10.7 $\pm$ 0.2	8.0 - 12.0
Cr	17.5 $\pm$ 0.9	18.0 - 20.0
Mn	1.18	2.0 max
P	0.014 $\pm$ 0.0005	0.045 max
S	0.020	0.03 max
Si	0.760	1.0 max

F. FLUENCE DETERMINATIONS

The pressure vessel wall was sampled for determination of fluence by drilling holes from the outside of the A350 steel wall, inward, with drillings from the desired depths saved for analysis. The analysis was performed by counting the Mn^{54} activity. In this way it was found that on the level of the reactor core midplane the fluence was approximately 9×10^{18} n/cm^2 in a region 0.95 cm (3/8 inch) from the inner edge of the A350 - LF3 steel vessel wall. On moving radially outward to a point 0.95 cm from the outer edge the fluence had fallen to about 4×10^{18} n/cm^2 E > 1 MeV.

IV. RESULTS OF MACRO AND FRACTOGRAPHIC EXAMINATION

A. INTERIOR REGION OF A350 - LF3 STEEL

For the purposes of this report the region of the A350 steel fracture surface exclusive of the stress corrosion and shear lip areas is defined as the interior region, and constitutes by far the majority of the area of the A350 fracture surface. Electron fractographs (some of which are reproduced in Figure 13) from all points sampled in this region showed the same characteristic, namely quasi-cleavage. From the macrophotographs and the fractographs it may be concluded that the fracture of the interior region of the A-350 steel was at least 90% brittle.

B. SHEAR LIPS

Fractographs from the shear lips showed surfaces completely, or almost completely, covered with dimples as illustrated in Figure 14. Trudeau[3] states that generally a brittle fracture in a ferritic steel is accompanied by shear lips to a certain extent. Dimpling is characteristic of a ductile fracture. From this it is apparent that the fracture process was almost completely ductile in the shear lip region, even though the majority of the A-350 steel failed by brittle fracture.

C. STAINLESS STEEL LINER

The stainless steel region produced fractographs (Figure 15) which were practically identical in appearance with those from the shear lip, i.e. a field completely or almost completely filled with dimples. Obviously the stainless steel was not embrittled by the fluence to which it had been exposed.

D. STRESS CORROSION REGION

The fractographs from the stress corrosion region (Figure 16) were the most difficult of all to interpret, probably because most of the features observed here were largely or entirely due to corrosion products. Figures 16A through 16D show both cleavage and corrosion products. In the region of the crack origin the relative thickness of the stainless steel weld overlay of 0.30 to 0.33 inch to that of the A350 - LF3 may have necessitated the depth (0.16 to 0.20 inch) of the stress corrosion required to start the running crack. The resultant thickness of the interior A350 - LF3 steel in the crack region was about the same as that of the stainless steel.

A. Region 4 of Figure 3. 3340 x.

B. Region 4 of Figure 3. 7980 x.

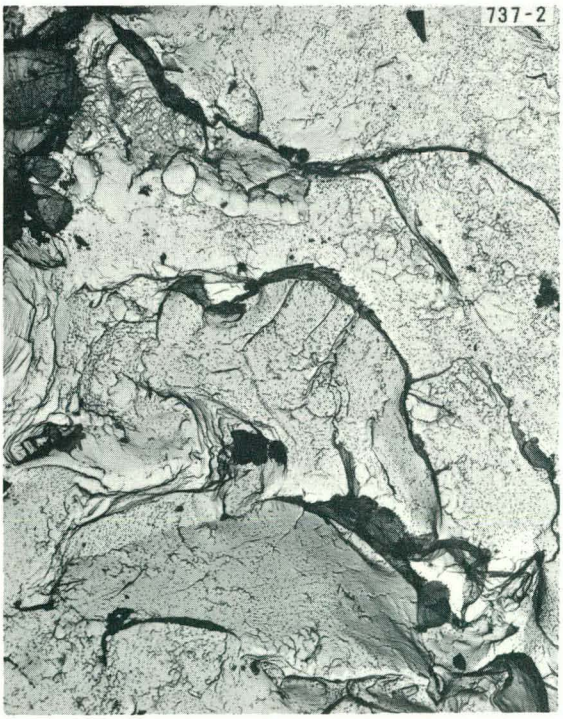

C. Region 8 of Figure 3. 3340 x.

D. Region 9 of Figure 3. 7980 x.

Electron Fractographs of Rapid Running Fracture Surface in A 350-LF3 Steel Showing Quasi-Cleavage

FIG 13.

(continued on next page)

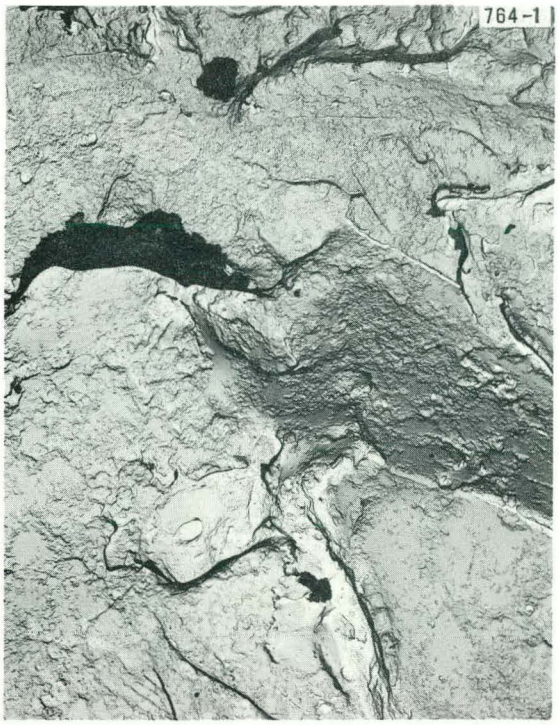

E. Region 1 of Figure 3. 3300 x.

F. Region 10 of Figure 3. 8200 x.

G. Region 5 of Figure 3. 3340 x.

H. Region 2 of Figure 3. 7980 x.

Electron Fractographs of Rapid Running Fracture Surface in A-350-LF3 Steel Showing Quasi-Cleavage.

FIG 13 (concluded)

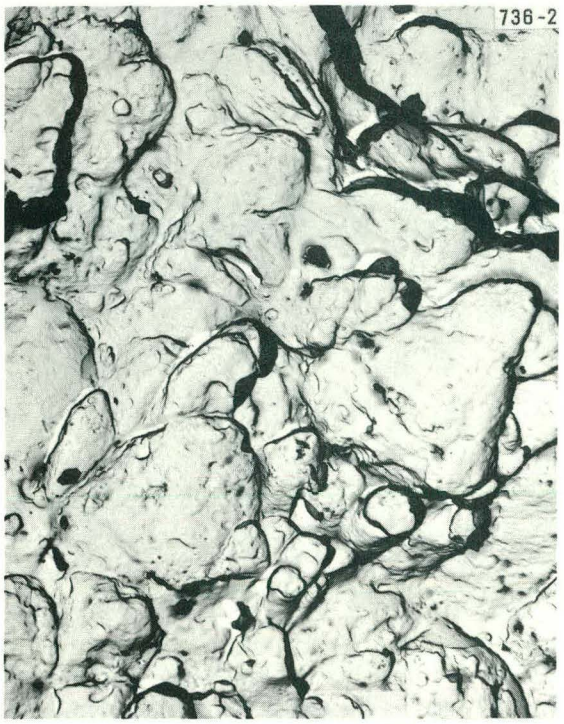

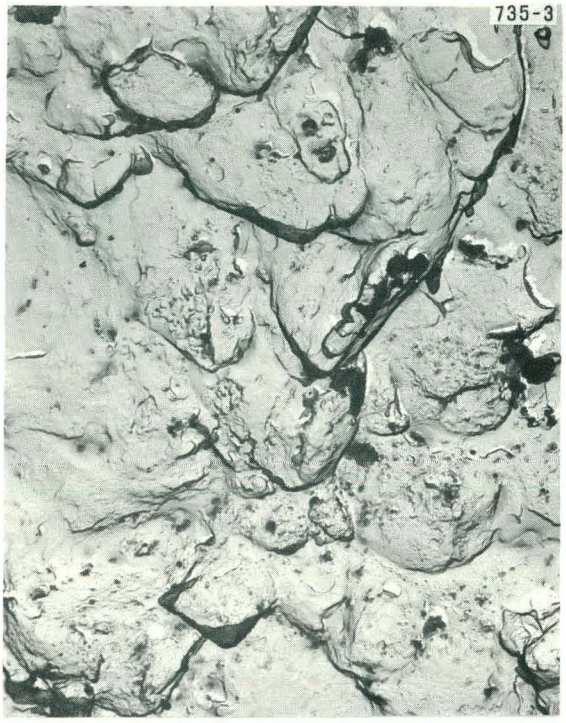

Electron Fractographs From Shear Lip From Region 8 of Figure 3. 7980 x.

FIG 14.

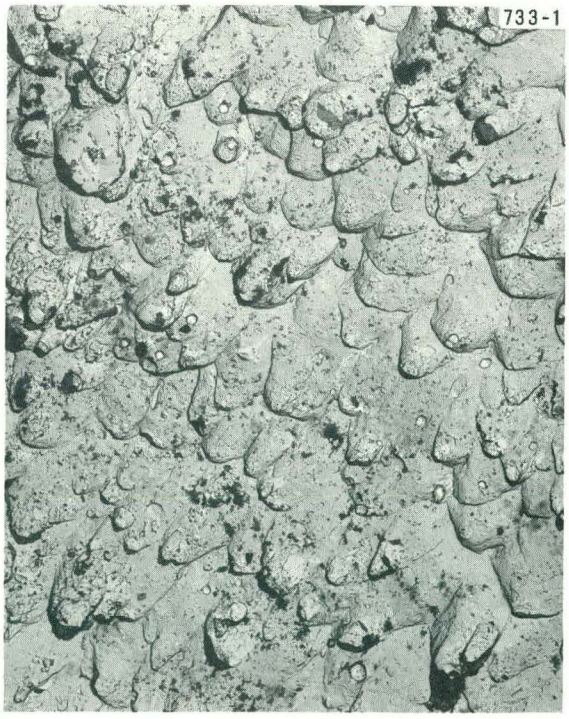

A. From Region 3 of Figure 3. 7980 x. B. From Region 4 of Figure 3. 3340 x.

Electron Fractographs From 304 Stainless Steel.

FIG 15.

A. 7980 x Both Cleavage Planes and Corrosion Products. B. 7980 x

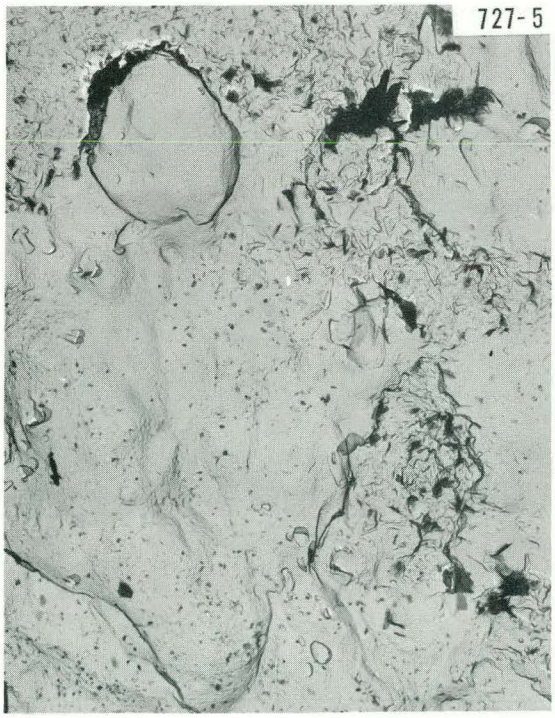

C. 7980 x. Principally Corrosion Products. D. 3340 x.

Electron Fractographs From Stress Corrosion Area, Region 4 of Figure 3.
FIG 16.

V. DISCUSSION

Stress corrosion cracking tests under similar conditions of temperature and stress had been performed[1] on notched samples from a sister forging prior to the stress corrosion of the PM-2A vessel. These tests gave a stress corrosion cracking rate of about 0.025 inches per hour. On this basis the stress corrosion depth of 0.16 to 0.20 inch observed in the irradiated PM-2A vessel is three to four times that which would have been expected. It may be speculated that the radiation exposure of the pressure vessel material could have rendered it more susceptible to stress corrosion cracking.

As has been discussed previously the interior region which constituted the great majority of the A350 fracture surface exhibited quasi-cleavage and hence represented a decidedly brittle fracture. This was due undoubtedly in part to the mode of fracture which enforced plane strain conditions and in part to the embrittling effect of irradiation on the steel. It has been estimated[4] that the NDT (nil ductility transition) temperature of the irradiated A350 steel was about 212°F, hence the destructive test at -20°F definitely was in a brittle temperature region.

No appreciable difference was noted in the nature of the rapid running fracture surface between the origin and the ends of the piece examined. From this it was concluded that the velocity of the rapid running crack did not change appreciably over the region examined, although the velocity would be expected to decrease as the crack terminated.

In contrast to the brittle A350 steel, the 304 stainless steel which had been subjected to the highest fluence due to its position immediately adjacent to the reactor core and also was subject to plane strain conditions showed a decidedly ductile behavior. This is not surprising since others[5,7] have found that 304 stainless steel is resistant to embrittlement by irradiation. They find this steel after irradiation to fluences of over 10^{19} n/cm^2 still was capable of over 30% elongation, that is to say it would be still decidedly ductile.

The ductile behavior indicated by the dimpling in the shear lip is possibly a different explanation. Trudeau's statement[3] to the effect that a brittle fracture in a ferritic steel is usually accompanied to a certain extent by shear lips already has been referred to. Beachem[6] explains this by saying that "as a flat running fracture approaches a free surface, one of the principal stresses at the tip of the fracture is relaxed sufficiently to cause fracture to be completed by an oblique shear lip". In this same reference he states that shear rupture leads to void coalescence and that fractures involving void coalescence have surfaces containing dimples. Thus, it would seem that the type and appearance of a fracture depends in part on the way in which the fracture was produced and in part on the inherent properties of the material.

The irradiation embrittlement in the outer wall (fluence < 4×10^{18} n/cm^2 in the region of the shear lip above and below the artificial defect) is minimal so that the ΔNDT is less than 160°F but probably greater than 50°F[8]. The radial cross section of the shear lip allows an estimation of a width and slant height of about 0.1 inch. A slight plastic contraction was noted in the shear lip in the plane of the vessel surface. Thus, the embrittlement though slight has

been overcome by the principal stress relaxation even though the test temperature of -20°F was below the NDT (of the irradiated steel approximately -10 to 100°F) and considerably below NDT + 60, the upper operating limit for prevention of brittle failure, so that the steel in the region of the shear lip was essentially brittle material.

It would be interesting to observe what percentage of elongation is shown by the tensile specimens prepared from the irradiated vessel wall and to compare their fracture surfaces with the PM-2A pressure vessel fracture.

VI. REFERENCES

1. J. M. Monahan and T. J. Walker, PM-2A Reactor Vessel Test - Description of Testing and Failure Conditions, WAPD TM-640 (January, 1967).

2. D. R. Mousseau and J. C. Pruden, PM-2A Reactor Vessel Test Program Final Report, IN-1061 (March 1967).

3. L. P. Trudeau, "Radiation Effects on Toughness of Ferritic Steels for Reactor Vessels", Rowan and Littlefield, Inc., New York, 1964

4. J. M. Monahan and P. A. Halpine, PM-2A Reactor Vessel Test - Phase I, WAPD-TM-604 (July 1966).

5. H. D. Gronbeck, ETR Radiation Damage Surveillance Programs Progress Report II, IN-1036 (February 1967).

6. C. D. Beachem, "Electron Fractographic Studies of Mechanical Fracture Processes in Metals", J. Basic Eng. 87, 299-306 (1965).

7. J. E. Irvin, A. L. Bement, and R. G. Hoagland, "The combined Effects of Temperature and Irradiation on the Mechanical Properties of Austentitic Stainless Steels", in ASTM STP 380, p. 236, (June 1965).

8. L. E. Steele and J. R. Hawthorne, "New Information on Neutron Embrittlement and Embrittlement Relief of Reactor Pressure Vessel Steels", in ASTM STP 380, p. 288 and 292.